Forecast of sector demand in multi-sector scenarios

Deliverable ID:	**D5.1**
Dissemination Level:	**PU**
Project Acronym:	**FMP-Met**
Grant:	**885919**
Call:	**H2020-SESAR-2019-2**
Topic:	**SESAR-ER4-05-2019 - Environment and Meteorology for ATM**
Consortium Coordinator:	**USE**
Edition Date:	**10 November 2021**
Edition:	**00.01.00**
Template Edition:	**02.00.02**

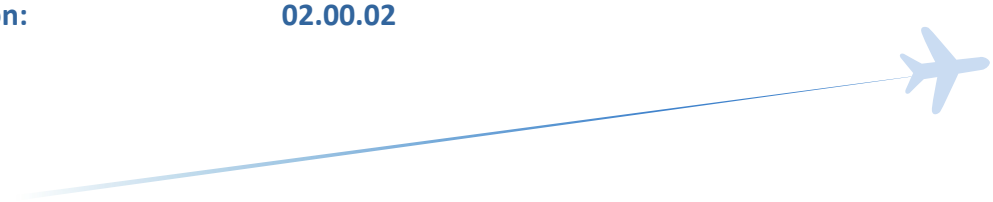

FMP-Met

METEOROLOGICAL UNCERTAINTY MANAGEMENT FOR FLOW MANAGEMENT POSITIONS

This deliverable is part of a project that has received funding from the SESAR Joint Undertaking under grant agreement No 885919 under European Union's Horizon 2020 research and innovation programme.

Abstract

This document presents the methodologies developed in work package 5 of the FMP-Met project regarding the probabilistic prediction of sector demand and congestion when convective weather is forecasted. These methodologies are required to fulfil the Concept of Operations devised in work package 2.

Firstly, a methodology to compute probabilistic forecasts of the entry and occupancy counts for individual sectors is presented. This methodology relies on the probabilistic aircraft trajectories returned by the trajectory predictors developed in work package 4. This methodology considers that multiple uncertainty sources may be present, and their statistical correlations. Secondly, a methodology to determine the probabilistic traffic overload of the sector is presented. This methodology considers the previous probabilistic counts and the weather-dependent capacities derived from the capacity reductions determined by work package 6 methodologies.

Results are shown for a realistic scenario, corresponding to a historical situation over the Austrian airspace on a day with significant convection.

Table of Contents

List of Figures

List of Tables

1 Introduction

1.1 FMP-Met project

The framework for the FMP-Met project is the integration of meteorological forecast uncertainty information into the decision-making process for the Flow Management Position (FMP), with the purpose of improving the understanding of adverse-weather effects on the Air Traffic Management (ATM) system and seeking ways to alleviate them. Its objective is to provide a probabilistic assessment of the impact of convective weather, useful for FMP (as the end user), intuitive and interpretable, to allow better-informed decision making.

The structure of the project is sketched in Figure 1, which consists of 6 different technical work packages (WPs). The Concept of Operations was developed in WP 2. This concept integrates probabilistic forecasts of traffic (entries and occupancies) and acceptable traffic load due to expected adverse weather in flow-management procedures. WP 3 dealt with the provision of the different probabilistic weather forecasts with different look-ahead times, namely probabilistic Nowcasts and Ensemble Prediction Systems (EPS). The trajectory prediction was addressed in WP 4. Two trajectory predictors were developed and integrated: a short-term trajectory predictor for the first hour, based on Nowcast, and a long-term trajectory predictor from 1 hour onwards up to 8 hours, based on EPS. The present work package, WP 5, deals with the provision of probabilistic forecasts of traffic counts, derived from the predicted trajectories, and congestion, by comparing the demand to weather-dependent capacity. In WP 6, the reduction of the available airspace capacity caused by convective weather is determined (WP 6.1), as well as the complexity coming from the interactions among flights and the adverse weather (WP 6.2). Finally, the concept is evaluated and assessed in WP 7.

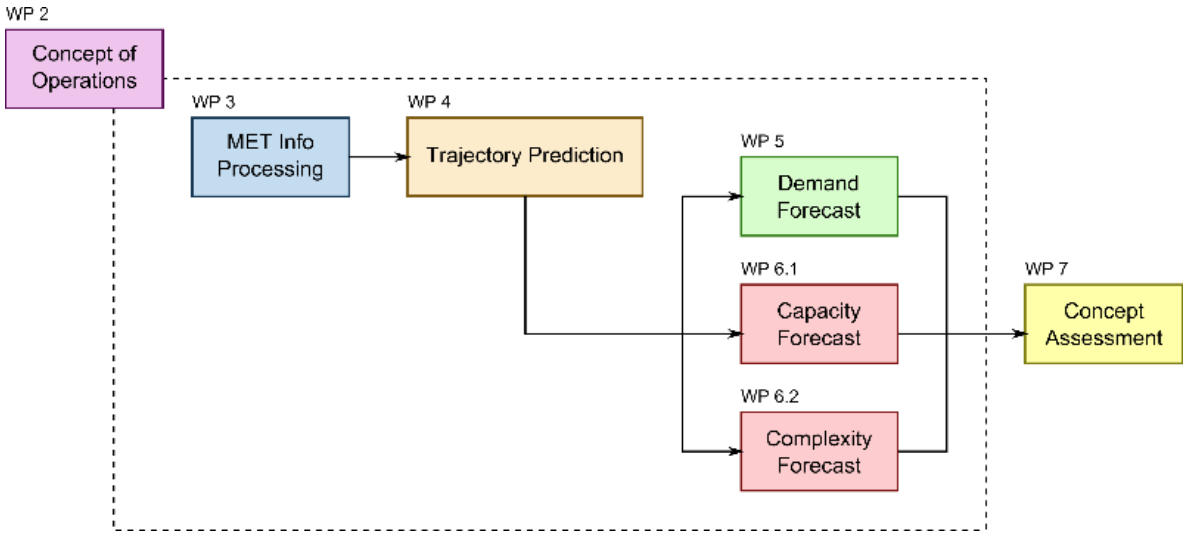

Figure 1: FMP-Met project structure.

1.2 Purpose and scope of this deliverable

Nowadays, the Network Manager supports FMPs with current and anticipated air traffic demand via Eurocontrol's CHMI (Collaboration Human Machine Interface) tool. These predictions are deterministic and based on data received from the flight-plan processing systems, airspace databases, live ATC (Air Traffic Control) data from ANSPs (Air Navigation Services Providers), aircraft operator's position reports, and meteorological data from a weather service provider.

The Concept of Operations developed in WP 2 [1] is an evolution of the current practice, which switches from deterministic predictions to probabilistic ones. It includes the use of a decision support tool composed of two main functions: probabilistic traffic and capacity forecasting and FMP measures evaluation. The probabilistic traffic and capacity forecasting consists of three main layers: *Traffic Volume Analysis View*, *Traffic Volume Monitor*, and *Sector Configuration Monitor*.

- The *Traffic Volume Analysis View* provides detailed insight into the situation in a specific traffic volume; it displays the traffic counts and the capacities based on the weather forecasts, and the probability distribution of the difference between demand and capacity.

- The *Traffic Volume Monitor* displays the traffic loads of the traffic volumes. The traffic load is represented by a color code, where each color represents its acceptability: green if the traffic load is acceptable, yellow if it is high, orange when very high, and red if unacceptable. The colors are determined by the probability of the demand exceeding different capacity thresholds.

- The *Sector Configuration Monitor* shows the time evolution of the demand-capacity balance for all sector configurations of interest. Again, it uses a color code to indicate how appropriate a sector configuration would be at a given time, and these colors are determined from the color state of its constituents traffic volumes: green if the traffic load is acceptable for all volumes, yellow if it is high for at least one volume, orange if it is very high for at least one volume, and red if it is unacceptable for at least one volume.

As it can be seen, these three layers rely on the computation of the stochastic distributions of the traffic counts and their differences with weather-dependent capacities. The methodologies required to perform these computations have been developed in WP 5 and are presented in this deliverable.

The work has been structured into two tasks: 1) provision of probabilistic forecasts of entry and occupancy counts for individual sectors, and 2) provision of probabilistic forecasts of the congestion of sector configurations.

In the first task, a methodology to compute the probability distributions of the entry and occupancy counts for individual sectors has been developed. The counts are determined from the probabilistic entry and exit times of all the aircraft that may cross the sector. These times are obtained from the probabilistic aircraft trajectories returned by the trajectory predictors developed in WP 4. This methodology considers that the trajectories are predicted using different weather products, that multiple uncertainty sources are present, and that these uncertainties may be correlated or uncorrelated. It also considers climbing/descending trajectories that may enter/exit the sector not only by the lateral but also by the vertical limits. Although the methodology has been developed for ATC sectors, it can be applied to any generic airspace or traffic volume. The work carried out in TBO-Met project [2] to predict sector demand has served as a starting point. These developments are presented in Section 2.

In the second task, a methodology to compute the probabilistic difference of the counts exceeding weather-dependent capacities, which will be referred as probabilistic overload, has been devised. The probabilistic entry and occupancy counts are those obtained in the previous task. The weather-dependent capacities are derived from the capacity reductions determined by WP 6 methodologies. Again, multiple uncertainty sources and their statistical correlations are considered. The probability of congestion of each individual sector can be readily obtained from the probabilistic overload. The developed methodology is presented in Section 3.

Finally, a realistic application of the previous methodologies is presented in Section 4. It corresponds to a historical situation over the Austrian airspace on a day with substantial convection.

1.3 Intended readership

This document is intended to be read by FMP-Met members, SJU (included the Commission Services), and ATM stakeholders.

1.4 Acronyms and Terminology

Acronym	Description
ACC	Area Control Centre
ANSP	Air Navigation Services Provider
ASCR	Available Sector Capacity Ratio
ATC	Air Traffic Control
ATM	Air Traffic Management
ECMWF	European Centre for Medium-Range Weather Forecasts
EPS	Ensemble Prediction System
FMP	Flow Management Position
MV	Monitoring Value
OTMV	Occupancy Traffic Monitoring Value
UTC	Coordinated Universal Time
WP	Work Package

1.5 FMP-Met Consortium

Acronym	Description
USE	Universidad de Sevilla
AEMET	Agencia Estatal de Meteorología
ACG	Austro Control GmbH
CCL	Croatia Control Limited
LiU	Linköping University
MetSol	MeteoSolutions GmbH
PLUS	Paris-Lodron Universität Salzburg
UC3M	Universidad Carlos III de Madrid
ZFOT	University of Zagreb

2 Prediction of entry and occupancy counts considering multiple uncertainty sources

This section presents the methodology developed to determine the probability distributions of the entry and occupancy counts for individual ATC sectors. First, some definitions are provided, and the general hypotheses are established. Second, the procedure to determine the time spent by a flight within an ATC sector, considering that multiple predicted trajectories are provided for each flight, is presented. Afterwards, the obtention of the probability distributions of the entry and occupancy counts from the previous times is described.

2.1 Definitions and general hypotheses

It is considered that the airspace under responsibility of the FMP is partitioned into a set of 3-dimensional volumes, each one of them is referred to as an elementary volume. The total number of elementary volumes is N_v, they are pairwise disjoint, and their union is equal to the airspace under responsibility of the FMP. Furthermore, ATC sectors are defined as a sub-set of adjacent elementary volumes. Finally, a sector configuration is a collection of ATC sectors that are pairwise disjoint and cover the airspace under responsibility of the FMP; hence, a sector configuration is a partition (in a mathematical sense) of the set of elementary volumes. In FMP-Met project, all the possible sector configurations, ATC sectors, and elementary volumes are given.

The sector demand and the congestion are predicted at a time, T_P, named as the prediction time. It is considered that the predicted trajectories and the weather-dependent sector capacities, required to obtain the demand and the congestion, are also predicted at this time, and they are obtained using the last available information (i.e., aircraft position reports, weather forecasts, etc.).

It is considered that there exist N_f different flights and that each flight is affected by several sources of uncertainty:

- The meteorological uncertainty, either linked to the future location of the convective cells or to the future temperature and wind fields (both inherent to the forecast process). The number of different weather ensemble members is denoted as N_w.
- The operational uncertainty linked to the storm avoidance strategy, as dictated by the topology of the field of storm cells (only in short-term trajectory prediction). The number of different avoidance strategies is denoted as N_a.
- The uncertainty in the initial condition, caused either by the uncertainty in the take-off time or by the uncertainty in the trajectory generated by a previously applied trajectory predictor. The number of initial conditions is denoted as N_i.

The approach followed in WP 4 was to produce an ensemble of trajectories corresponding to a single flight that represents the effects of these uncertainty sources [3]. However, as the various weather forecasts apply at different time frames and coverage areas, the unified framework for trajectory prediction provides a piecewise description of the predicted trajectory, i.e., the flight is composed of several flight legs. Each leg contains an ensemble of pieces of trajectories obtained by applying a specific trajectory predictor.

Among the legs obtained for a single flight, only those computed either with the Nowcast-based trajectory predictor or the COSMO-based trajectory predictor are of interest for the purposes of traffic demand forecasting. It leads to every flight having either a single leg (a Nowcast-based leg or a COSMO-based leg) or two legs (both a Nowcast-based one and a COSMO-based one). The Nowcast-based legs are used for traffic demand computations from the prediction time, T_P, to the transition time between the two weather products, $T_T = T_P + 1$ hour, whereas the COSMO-based legs are used for traffic demand computations from T_T to the maximum look ahead time, $T_P + 8$ hours.

For different flights within the same time frame (either from T_P to T_T or from T_T to $T_P + 8$ hours), it is assumed that the meteorological uncertainty is fully correlated (as they all share the same weather information) whereas the uncertainty in the initial conditions and in the operational uncertainty (if applicable) are statistically independent from one flight to another. Therefore, it is useful to refer to each trajectory ensemble member by using not just one index, but two indices: k ($k = 1, \dots, N_w$) for the weather ensemble member considered, and l ($l = 1, \dots, N_u$, where either $N_u = N_a N_i$ or $N_u = N_i$) for the combination of uncorrelated uncertainty sources.

The position of flight i ($i = 1, \dots, N_f$) for weather ensemble member k ($k = 1, \dots, N_w$) and uncorrelated uncertainty member l ($l = 1, \dots, N_u$) at time t, is denoted as $\mathbf{x}_i^{[k,l]}(t)$. It is given by the longitude λ, the latitude ϕ, and the pressure altitude h:

$$\mathbf{x}_i^{[k,l]}(t) = \left[\lambda_i^{[k,l]}(t), \phi_i^{[k,l]}(t), h_i^{[k,l]}(t)\right]. \tag{1}$$

The trajectories $\mathbf{x}_i^{[k,l]}$ generated by the trajectory predictor are provided as a list of discrete points and times; when needed, a linear interpolation is used to obtain the position of the flight at any time.

2.2 Time spent inside an ATC sector

To obtain the time spent by each flight inside an ATC sector, first the set of entry and exit times to/from the elementary volumes is determined. The reason to perform this intermediate step, instead of directly computing the entry and exit times to/from the sector, is twofold. In the first place, the elementary volumes usually present a simpler geometry than the ATC sectors (elementary volumes usually are right prisms while ATC sectors may present some balconies), which simplifies the geometrical computations and the robustness of the implementation. Secondly, the number of elementary volumes in the airspace under FMP's responsibility is usually smaller than the number of sectors, which reduces the number of mathematical operations and improves the computational efficiency. The intersections with the elementary volumes are computed once and the times spent inside the sectors for all configurations are obtained by combining these results. The devised procedure is described next.

If a trajectory $\mathbf{x}_i^{[k,l]}$ crosses an elementary volume, then there is a non-empty set of time instants at which the aircraft is predicted to be inside that elementary volume. In the more general case, the time spent by a flight i ($i = 1, \dots, N_f$) for weather ensemble member k ($k = 1, \dots, N_w$) and uncorrelated uncertainty member l ($l = 1, \dots, N_u$) inside an elementary volume v ($v = 1, \dots, N_v$) is given by

$$T_{iv}^{[k,l]} = \bigcup_{r=1}^{R} \left[t_{iv,E_r}^{[k,l]}, t_{iv,X_r}^{[k,l]}\right], \tag{2}$$

where the trajectory is assumed to cross the elementary volume several times (particularly, R times), entering at $t_{iv,E_r}^{[k,l]}$ and exiting at $t_{iv,X_r}^{[k,l]}$. The aircraft may enter/exit the elementary volume through either its lateral sides or its top/bottom faces.

Analogously, if a trajectory $\mathbf{x}_i^{[k,l]}$ crosses the airspace under responsibility of the FMP, then there is a non-empty set of time instants at which the aircraft is predicted to be inside that airspace. In this case, to obtain the time spent by a flight i ($i = 1, \dots, N_f$) for weather ensemble member k ($k = 1, \dots, N_w$) and uncorrelated uncertainty member l ($l = 1, \dots, N_u$) inside sector s of a given sector configuration, one must compute the Boolean union of the time spent inside each of the constituting elementary volumes (i.e., $v \in I_s$, where I_s is the set of elementary volumes forming the sector s):

$$T_{is}^{[k,l]} = \bigcup_{v \in I_s} T_{iv}^{[k,l]}. \tag{3}$$

Once it is computed, it will have the following structure

$$T_{is}^{[k,l]} = \bigcup_{q=1}^{Q} \left[t_{is,E_q}^{[k,l]}, t_{is,X_q}^{[k,l]} \right], \tag{4}$$

where the trajectory is assumed to cross the sector several times (particularly, Q times), entering at $t_{is,E_q}^{[k,l]}$ and exiting at $t_{is,X_q}^{[k,l]}$.

A high-level conceptual description of the procedure followed to calculate the sequence of time intervals $\left[t_{is,E_q}^{[k,l]}, t_{is,X_q}^{[k,l]} \right]$ through all the ATC sectors in a desired set of sector configurations is sketched in Figure 2. The whole procedure is organized in two blocks, as described previously. The inputs are the geometries of the elementary volumes, the ensemble of predicted trajectories, and the definition of the sector configurations. The output is the ensemble of time intervals spent inside every sector.

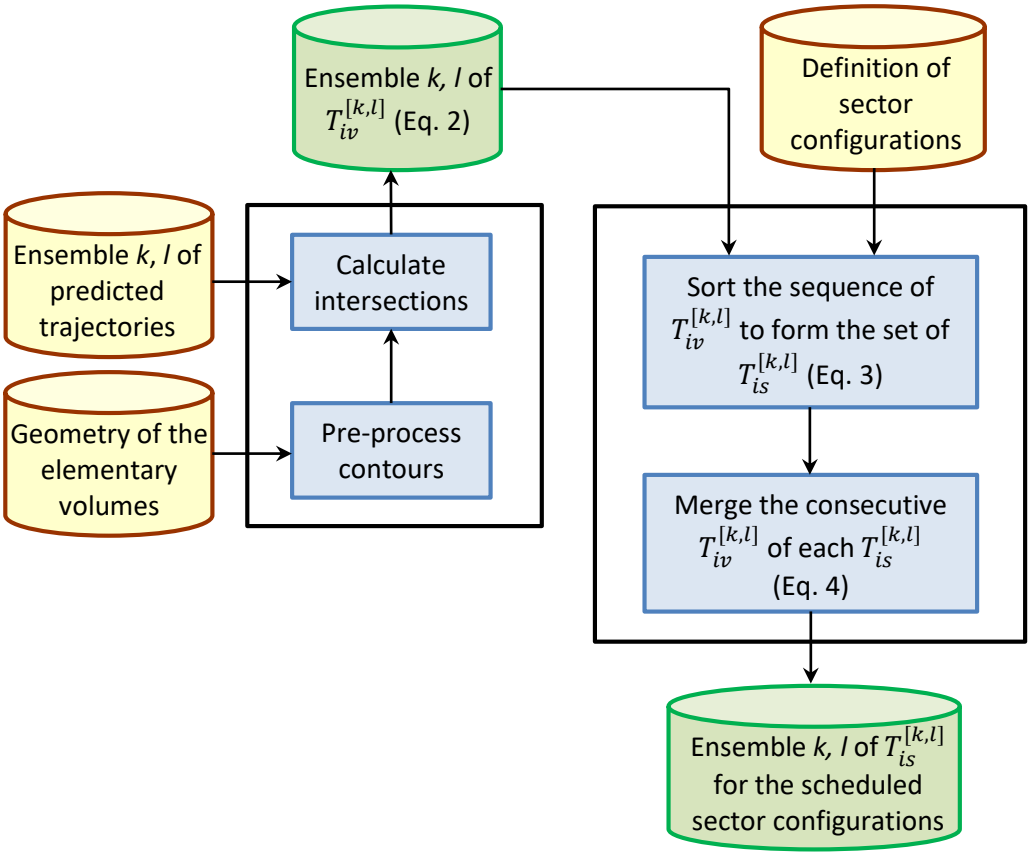

Figure 2: High-level description of the procedure to calculate sector's entry and exit times.

2.3 Entry count

The entry count for a given sector is defined as the number of flights entering the sector during a selected time period P_j,

$$P_j = [T_P + (j-1)\delta t, T_P + (j-1)\delta t + \Delta t), \qquad j = 1,2,\ldots, \tag{5}$$

Where T_P is the time at which the prediction is performed, δt is the time step, i.e., the difference between the start times of two consecutive time periods, and Δt is the duration of each period. In practice, the time step is a submultiple of the duration (which includes the particular case that $\delta t = \Delta t$, but is not restricted to it).

Because the time spent inside a sector is uncertain, the aircraft can enter the sector in different time periods, thus leading to an uncertain entry count. The larger the dispersion of the entry time and the smaller the values of Δt, the more likely the entry count to be uncertain. For example, in case that the dispersion of the entry time of one flight is larger than the duration of the time period, then this flight may enter the sector in two or more consecutive time periods.

When computing the entry count of a sector, it is common practice not to consider flights spending a short time within it. In fact, this can be configured in the Network Manager's monitoring tool CHMI (CIFLO for an FMP) through a parameter called SKIP-IN, namely, $\Delta t_{SKIP-IN}$. Additionally, to avoid

double-counting of re-entry flights, it is also common to ignore an entry of a flight to a sector when it has already been counted and has left the sector some time ago. In CIFLO, this can be configured through the SKIP-OUT parameter, namely, $\Delta t_{SKIP-OUT}$. According to these concepts, an entry with associated entry and exit times $t_{is,E_q}^{[k,l]}$ and $t_{is,X_q}^{[k,l]}$, respectively, is said to contribute to the entry count if the following two conditions hold:

1) $t_{is,X_q}^{[k,l]} - t_{is,E_q}^{[k,l]} \geq \Delta t_{SKIP-IN}$.
2) $t_{is,E_q}^{[k,l]} - t_{is,X_w}^{[k,l]} \geq \Delta t_{SKIP-OUT}$ for all the previous entries (i.e., $w < q$) that contribute to the entry count.

Note that this is a recursive definition, so it must be sequentially applied, starting from the first entry (for which the SKIP-OUT condition is considered to hold). For convenience, the entry time associated to an entry that contributes to the entry count will be renamed as $\hat{t}_{is,E_q}^{[k,l]}$.

We define an entry function for flight i, for weather ensemble member k, for uncorrelated uncertainty member l, for sector s, and for time period P_j, denoted as $E_{sj}^{[k,i,l]}$. It takes the value 1 when the aircraft enters the ATC sector (through a contributing entry) at least once during this period and the value 0 otherwise:

$$E_{sj}^{[k,i,l]} = \begin{cases} 1, & \text{if } \exists q : \hat{t}_{is,E_q}^{[k,l]} \in P_j \\ 0, & \text{otherwise.} \end{cases} \tag{6}$$

Note that if the aircraft does not enter the ATC sector, $E_{sj}^{[k,i,l]}$ is set to zero even though $\hat{t}_{is,E_q}^{[k,l]}$ is not defined. Furthermore, if the aircraft enters the ATC sector more than once (which is not prevented by the SKIP-OUT condition when $\Delta t_{SKIP-OUT} < \Delta t$), $E_{sj}^{[k,i,l]}$ is set to one, no matter how many times it does so.

The event that the flight i enters the ATC sector s at period P_j for the weather ensemble member k can be modelled as a random variable with a Bernoulli distribution, with parameter the probability $p_{sj,E}^{[k,i]}$. This probability $p_{sj,E}^{[k,i]}$ is estimated from the values of the entry function, according to the following expression:

$$p_{sj,E}^{[k,i]} = \frac{1}{N_u} \sum_{l=1}^{N_u} E_{sj}^{[k,i,l]}. \tag{7}$$

The corresponding probability mass function can be formulated as follows [4]:

$$p_{sj,E}^{[i]}(z|k) = \begin{cases} 1 - p_{sj,E}^{[k,i]}, & \text{if } z = 0 \\ p_{sj,E}^{[k,i]}, & \text{if } z = 1, \end{cases} \tag{8}$$

where $z = 1$ represents that the aircraft enters the sector, and $z = 0$ that it does not enter.

Since the random variables corresponding to different flights are statistically independent, the total amount of flights entering the ATC sector s at period P_j for the weather ensemble member k is a random variable $E_{sj}^{[k]}$ following a Poisson binomial distribution. The corresponding probability mass function $p_{s_{j,E}}(e|k)$, with $e \in \{0,1,2 \dots, N_f\}$, is obtained from the convolution of the probability mass functions of the flights involved [5], that is, $p_{sj,E}^{[i]}(z|k)$ for $i = 1, \dots, N_f$.

Once the probability distribution of the total amount of flights entering the ATC sector s at period P_j for each weather ensemble member has been computed, the marginal distribution is obtained by marginalizing over the weather ensemble members. Considering the general relation between the conditional and the marginal probabilities [4] and assuming the different weather ensemble members to be equally likely ($p_K(k) = \frac{1}{N_w}$), one can conclude that the total amount of flights entering the ATC sector s at period P_j, namely E_{sj}, is given by the following probability mass function:

$$p_{sj,E}(e) = \frac{1}{N_w} \sum_{k=1}^{N_w} p_{sj,E}(e|k). \tag{9}$$

Since the entry count is usually measured over long time periods (e.g., one hour) and with $\delta t < \Delta t$, it is common that the period P_j contains the transition time between the two weather products and trajectory predictors, T_T (recall that, in this project, $T_T = T_P + 1$ hour). When this situation occurs, a modified procedure has to be defined to compute the entry count, as one can no longer identify a weather ensemble member all along the time period. The modified procedure is based on the idea that the entry count over a period $A = B \cup C$ equals the sum of the entry count over B and the entry count over C. Hence, if P_j contains T_T, the time period is first broken into two pieces

$$P_{j,-} = [T_P + (j-1)\delta t, T_T), \qquad P_{j,+} = [T_T, T_P + (j-1)\delta t + \Delta t). \tag{10}$$

Then, the probabilistic entry count is determined separately in both subperiods following the original procedure above, what leads to $p^-_{sj,E}(e)$ and $p^+_{sj,E}(e)$. Finally, these results are combined; specifically, assuming that both entry counts are independent, the total amount of flights entering the ATC sector s at period P_j, namely E_{sj}, follows a probability mass function $p_{sj,E}(e)$ obtained from the convolution of the probability mass functions $p^-_{sj,E}(e)$ and $p^+_{sj,E}(e)$ [5].

2.4 Occupancy count

The occupancy count for a given sector is defined as the number of flights inside the sector during a selected time period P_j, defined as before, see Eq. (5). As in the case of the entry count, since the time spent inside a sector is uncertain, the aircraft can enter or exit the sector in different time periods, and therefore the occupancy count is also uncertain.

When computing the occupancy count, it is common practice not to consider flights spending a short time within it, the same way as those flights were not considered to contribute to the entry count. Hence a stay with associated entry and exit times $t^{[k,l]}_{is,E_q}$ and $t^{[k,l]}_{is,X_q}$, respectively, is said to contribute to the occupancy count if the following condition holds: $t^{[k,l]}_{is,X_q} - t^{[k,l]}_{is,E_q} \geq \Delta t_{SKIP-IN}$. Now, for the occupancy count, a SKIP-OUT condition is not defined. Again, for convenience, the entry and exit times associated to a stay that contributes to the occupancy count will be renamed as $\check{t}^{[k,l]}_{is,E_q}$ and $\check{t}^{[k,l]}_{is,X_q}$, respectively.

Analogously, we define an occupancy function for flight i, for weather ensemble member k, for uncorrelated uncertainty member l, for sector s, and for period P_j, denoted as $O^{[k,i,l]}_{sj}$. It takes the value 1 when the aircraft is inside the ATC sector during this time period (it enters, exits, or stays in the sector in this period) and the value 0 if the aircraft is outside:

$$O_{sj}^{[k,i,l]} = \begin{cases} 1, & \text{if } \left(\exists q : \check{t}_{is,E_q}^{[k,l]} \in P_j\right) \text{ or } \left(\exists q : \check{t}_{is,X_q}^{[k,l]} \in P_j\right) \text{ or} \\ & \left(\exists q : \check{t}_{is,E_q}^{[k,l]} < T_P + (j-1)\delta t \text{ and } \check{t}_{is,X_q}^{[k,l]} \geq T_P + (j-1)\delta t + \Delta t\right), \\ 0, & \text{otherwise.} \end{cases} \quad (11)$$

The event that the flight i is inside the ATC sector s at period P_j for the weather ensemble member k can be modelled as a random variable with a Bernoulli distribution, with parameter the probability $p_{sj,O}^{[k,i]}$. This probability $p_{sj,O}^{[k,i]}$ is estimated from the values of the occupancy function, according to the following expression:

$$p_{sj,O}^{[k,i]} = \frac{1}{N_u} \sum_{l=1}^{N_u} O_{sj}^{[k,i,l]}. \quad (12)$$

The corresponding probability mass function can be formulated as follows:

$$p_{sj,O}^{[i]}(z|k) = \begin{cases} 1 - p_{sj,O}^{[k,i]}, & \text{if } z = 0 \\ p_{sj,O}^{[k,i]}, & \text{if } z = 1, \end{cases} \quad (13)$$

where $z = 1$ represents that the aircraft does occupy the sector, and $z = 0$ that it does not.

Since the random variables corresponding to different flights are statistically independent, the total amount of flights inside the ATC sector s at period P_j for the weather ensemble member k is a random variable $O_{sj}^{[k]}$ following a Poisson binomial distribution. The corresponding probability mass function $p_{sj,O}(o|k)$, with $o \in \{0,1,2 \dots, N_f\}$, is obtained from the convolution of the probability mass functions of the flights involved, that is, $p_{sj,O}^{[i]}(z|k)$ for $i = 1, \dots, N_f$.

Once the probability distribution of the total amount of flights inside the ATC sector s at period P_j for each weather ensemble member has been computed, the marginal distribution is obtained by marginalizing over the weather ensemble members. Again, considering the general relation between the conditional and the marginal probabilities and assuming the different weather ensemble members to be equally likely, one can conclude that the total amount of flights inside the ATC sector s at time period P_j, namely O_{sj}, is given by the following probability mass function:

$$p_{sj,O}(o) = \frac{1}{N_w} \sum_{k=1}^{N_w} p_{sj,O}(o|k). \quad (14)$$

The occupancy count is usually measured over very short time periods (e.g., 1 minute) and with $\delta t = \Delta t$. In this case, it does not happen that the period P_j contains the transition time, T_T, and a modified methodology to cover this situation is not needed.

3 Sector congestion analysis

The *Traffic Volume Analysis View* proposed in Deliverable 2.1 [1] requires the computation of the absolute and relative differences between the traffic flow and the capacity. These differences will be named in this document as absolute and relative overloads.

Let us call TF_{sj} the traffic flow for ATC sector s and time period P_j, and Wx_Cap_{sj} the weather-dependent capacity for the same sector and period. The traffic flow can be either the entry count, $TF_{sj} = E_{sj}$, or the occupancy count, $TF_{sj} = O_{sj}$. The weather-dependent capacity must be then in accordance: If the traffic flow is the entry count, then the capacity becomes a weather-dependent monitoring value (MV), $Wx\_Cap_{sj} = Wx\_MV_{sj}$; if the traffic flow is the occupancy count, then it is a weather-dependent occupancy traffic monitoring value (OTMV), $Wx\_Cap_{sj} = Wx\_OTMV_{sj}$.

For sector s and period P_j, the absolute overload is defined as

$$AOL_{sj} = TF_{sj} - Wx\_Cap_{sj} \tag{15}$$

and the relative overload as

$$ROL_{sj} = TF_{sj}/Wx\_Cap_{sj}. \tag{16}$$

The *Traffic Volume Monitor* requires to compute the probability of the absolute or the relative overload being below predefined thresholds, i.e., $P[AOL_{sj} \leq \delta]$ or $P[ROL_{sj} \leq \varepsilon]$, where δ and ε are the thresholds.

Next, in Section 3.1, it is shown how the weather-dependent capacity Wx_Cap_{sj} is obtained from the available sector capacity ratios determined with the methodologies developed in WP 6. Afterwards, in Section 3.2, the absolute and relative overloads are determined for both the entries and the occupancies.

3.1 Weather-dependent capacity

WP 6 outputs the prediction of available sector capacity ratios (ASCRs). The ASCR is the ratio of the sector capacity under the given weather constraints to the maximum possible capacity of the sector without weather systems. The ratio is a non-dimensional value ranging between 0 and 1, where 0 represents a completely blocked airspace with no usable capacity and 1 represents an airspace without any weather-induced capacity reduction.

For each ATC sector s and weather ensemble member k, the ASCR is provided at discrete times. A right-continuous step function is created from these values, let's denote it as $ASCR_s^{[k]}(t)$; i.e., a piecewise constant function whose value at time t is the ASCR value provided for the immediately prior discrete time.

Since the ASCR may take different values while in one time period P_j, we define the mean ASCR for period j, $\overline{ASCR}_{sj}^{[k]}$, as a representative value of the sector status in that said period. It is obtained as follows:

$$\overline{ASCR}_{sj}^{[k]} = \frac{1}{\Delta t}\int_{T_P+(j-1)\delta t}^{T_P+(j-1)\delta t+\Delta t} ASCR_s^{[k]}(t)dt. \quad (17)$$

Gathering the results for all weather members, one obtains a stochastic mean status of the sector, $\overline{ASCR}_{sj}$, which follows a categorical distribution; its corresponding probability mass function is $p_{sj,\overline{ASCR}}(x) = 1/N_w$, with $x \in \left\{\overline{ASCR}_{sj}^{[1]}, \overline{ASCR}_{sj}^{[2]}, \dots, \overline{ASCR}_{sj}^{[N_w]}\right\}$.

The weather-dependent MV and OTMV for ensemble member k are obtained by multiplying the nominal monitoring values by the mean ASCRs:

$$Wx\_MV_{sj}^{[k]} = \overline{ASCR}_{sj}^{[k]} MV_s, \quad (18)$$

$$Wx\_OTMV_{sj}^{[k]} = \overline{ASCR}_{sj}^{[k]} OTMV_s. \quad (19)$$

In the above expressions, MV_s and $OTMV_s$ are the MV and the OTMV of sector s for the duration of the time period Δt, respectively; for example, MV per 60 minutes if Δt=60 minutes, or OTMV per 1 minute if Δt=1 minute.

Finally, gathering results for all members, one gets the aggregated weather-dependent capacities

$$Wx\_MV_{sj} = \overline{ASCR}_{sj} MV_s, \quad (20)$$

$$Wx\_OTMV_{sj} = \overline{ASCR}_{sj}\ OTMV_s. \quad (21)$$

It is worth noting that, as discussed in Section 2.3, when one has long time periods (e.g., one hour) and with $\delta t < \Delta t$, it is common that the period P_j contains the transition time between the two weather products, T_T. When this happens, it is not possible to obtain $\overline{ASCR}_{sj}^{[k]}$ because there is no correspondence between the weather members of the two weather products; that is, Eq. (16) cannot be longer applied. In that case, $\overline{ASCR}_{sj}$ is computed in a different way. First, the mean ASCR is determined separately before and after the transition time, and then these results are combined.

Before the transition time T_T, one has

$$\overline{ASCR}_{sj,-}^{[k]} = \frac{1}{T_T - T_P + (j-1)\delta t}\int_{T_P+(j-1)\delta t}^{T_T} ASCR_{sj}^{[k]}(t)dt \qquad \text{for } k = 1, \dots, N_{w1} \quad (22)$$

and $\overline{ASCR}_{sj,-}$ follows a categorical distribution with a probability mass function $p_{sj,\overline{ASCR}_-}(x) = 1/N_{w1}$, and $x \in \left\{\overline{ASCR}_{sj,-}^{[1]}, \overline{ASCR}_{sj,-}^{[2]}, \dots, \overline{ASCR}_{sj,-}^{[N_{w1}]}\right\}$. After the transition time T_T, one has

$$\overline{ASCR}_{sj,+}^{[k]} = \frac{1}{T_P + (j-1)\delta t + \Delta t - T_T}\int_{T_T}^{T_P+(j-1)\delta t+\Delta t} ASCR_{sj}^{[k]}(t)dt \qquad \text{for } k = 1, \dots, N_{w2} \quad (23)$$

and $\overline{ASCR}_{sj,+}$ also follows a categorical distribution with a probability mass function $p_{sj,\overline{ASCR}_+}(x) = 1/N_{w2}$, and $x \in \left\{\overline{ASCR}_{sj,+}^{[1]}, \overline{ASCR}_{sj,+}^{[2]}, \dots, \overline{ASCR}_{sj,+}^{[N_{w2}]}\right\}$. The mean ASCR for the sector, $\overline{ASCR}_{sj}$, is then obtained as a weighted sum of the two mean ASCRs

$$\overline{ASCR}_{sj} = \frac{T_T - T_P + (j-1)\delta t}{\Delta t}\overline{ASCR}_{sj,-} + \frac{T_P + (j-1)\delta t + \Delta t - T_T}{\Delta t}\overline{ASCR}_{sj,+} \quad (24)$$

Since the two addends are independent random variables, the probability mass function of $\overline{ASCR}_{sj}$ is obtained as the convolution of these two terms.

3.2 Absolute and relative overloads

Absolute overload

The absolute overload for ATC sector s, time period P_j, and ensemble member k is obtained as

$$AOL_{sj}^{[k]} = TF_{sj}^{[k]} - Wx\_Cap_{sj}^{[k]}. \tag{25}$$

Since $Wx\_Cap_{sj}^{[k]}$ is a deterministic value, $AOL_{sj}^{[k]}$ is simply the random variable $TF_{sj}^{[k]}$ shifted the amount determined by $Wx\_Cap_{sj}^{[k]}$. Its probability mass function is

$$p_{sj,AOL}(a^{[k]}|k) = p_{sj,TF}\left(a^{[k]} + Wx\_Cap_{sj}^{[k]}|k\right), \tag{26}$$

with $a^{[k]} \in \left\{a_i^{[k]}\right\}$, $a_i^{[k]} = i - Wx\_Cap_{sj}^{[k]}, i = 0,1,\dots,N_f$.

Once the probability distribution of the absolute overload of sector s at period P_j for each weather ensemble member has been computed, the marginal distribution is obtained by marginalizing over the weather ensemble members. Again, considering the general relationship between the conditional and the marginal probabilities and assuming the different weather ensemble members to be equally likely, one can conclude that the absolute overload of ATC sector s at period P_j, namely AOL_{sj}, follows the probability mass function:

$$p_{sj,AOL}(a) = \frac{1}{N_w}\sum_{k=1}^{N_w} p_{sj,AOL}(a|k) \text{ with } a \in \left\{a^{[1]}, a^{[2]}, \dots, a^{[k]}\right\}. \tag{27}$$

As before, when the period P_j encompasses the transition time between the two weather products, T_T, it is not possible to obtain $AOL_{sj}^{[k]}$ because there is no correspondence between the members of the two weather products. In that case, AOL_{sj} is computed assuming that TF_{sj} and Wx_Cap_{sj} are statistically independent. Hence, $AOL_{sj} = TF_{sj} - Wx\_Cap_{sj}$, and the probability mass function of AOL_{sj} is obtained as the convolution of the two addends.

Relative overload

The relative overload for ensemble member k is obtained as

$$ROL_{sj}^{[k]} = \frac{TF_{sj}^{[k]}}{Wx\_Cap_{sj}^{[k]}}. \tag{28}$$

Since $Wx\_Cap_{sj}^{[k]}$ is a deterministic value, $ROL_{sj}^{[k]}$ is just the random variable $TF_{sj}^{[k]}$ scaled by $Wx\_Cap_{sj}^{[k]}$. Its probability mass function is

$$p_{sj,ROL}(r^{[k]}|k) = p_{sj,TF}\left(r^{[k]}Wx\_Cap_{sj}^{[k]}|k\right), \tag{29}$$

with $r^{[k]} \in \left\{r_i^{[k]}\right\}$, $r_i^{[k]} = i/Wx\_Cap_{sj}^{[k]}, i = 0,1,\dots,N_f$.

As described before with the absolute overload, once the probability distribution of the relative overload of sector s at period P_j for each weather ensemble member has been obtained, the marginal distribution is obtained by marginalizing over the weather ensemble members. The relative overload of ATC sector s at period P_j, namely ROL_{sj}, follows the following probability mass function:

$$p_{sj,ROL}(r) = \frac{1}{N_w}\sum_{k=1}^{N_w} p_{sj,ROL}(r|k) \text{ with } r \in \left\{r^{[1]}, r^{[2]}, \dots, r^{[k]}\right\}. \quad (30)$$

As previously addressed, when the period P_j encompasses the transition time between the two weather products, it is not possible to obtain $ROL_{sj}^{[k]}$ because there is no correspondence between the members of the two weather products. In that case, ROL_{sj} is computed assuming again that TF_{sj} and Wx_Cap_{sj} are statistically independent. Hence, $ROL_{sj} = TF_{sj}/Wx\_Cap_{sj}$, and the probability mass function of ROL_{sj} is obtained as the Mellin convolution of the two terms [6].

4 Application

In this section, the previously described methodologies are applied to a historical situation over the Austrian airspace on 12th June 2018, a day with significant convection between 10:30 and 22:45 UTC (note that all times below are UTC). The prediction time is T_P =12:00. The scenario is described in Section 4.1, the entry and the occupancy counts are shown in Section 4.2, the weather-dependent capacities in Section 4.3, and the congestion in Section 4.4.

The methodologies have been implemented using the Python programming language. In particular, the Shapely Python package [7] has been used for the manipulation and operation of geometric objects such as points, lines, and polygons. It is based on the GEOS (Geometry Engine – Open Source) library [8], which is, in turn, a C++ port of the JTS Topology Suite (JTS) [9].

The following FMP-Met partners have provided the required input: ACG has provided the airspace data; AEMET, MetSol and UC3M have provided the probabilistic meteorological information according to the methodologies described in Deliverable 3.1 [10]; UC3M and USE have provided the probabilistic predicted trajectories according to the methodologies described in Deliverable 4.1 [3]; and LiU has provided the probabilistic available sector capacity ratios as described in Deliverable 6.1 [11].

4.1 Scenario

4.1.1 Airspace

For AIRAC cycle 1806, the Austrian airspace under the control of the Wien Area Control Centre (ACC WIEN) is shown in Figure 3. It is divided into five geographical regions (B, E, N, S and W), and each region into five vertical layers:

- ACC WIEN B: B1, B2, B3, B4, and B5;
- ACC WIEN E: E1, E2, E3, E4, and E5;
- ACC WIEN N: N1, N2, N3, N4, and N5;
- ACC WIEN S: S1, S2, S3, S4, and S5; and
- ACC WIEN W: W1, W2, W3, W4, and W5.

In total, 38 elementary volumes are used to define this airspace, which lead to near 60 possible different ATC sectors and 190 different sector configurations. For instance, sector configuration 2A is formed by two ATC sectors: SC15, which is formed by all the elementary volumes from ACC WIEN B, S and W; and NE15, formed by all the elementary volumes from ACC WIEN N and E.

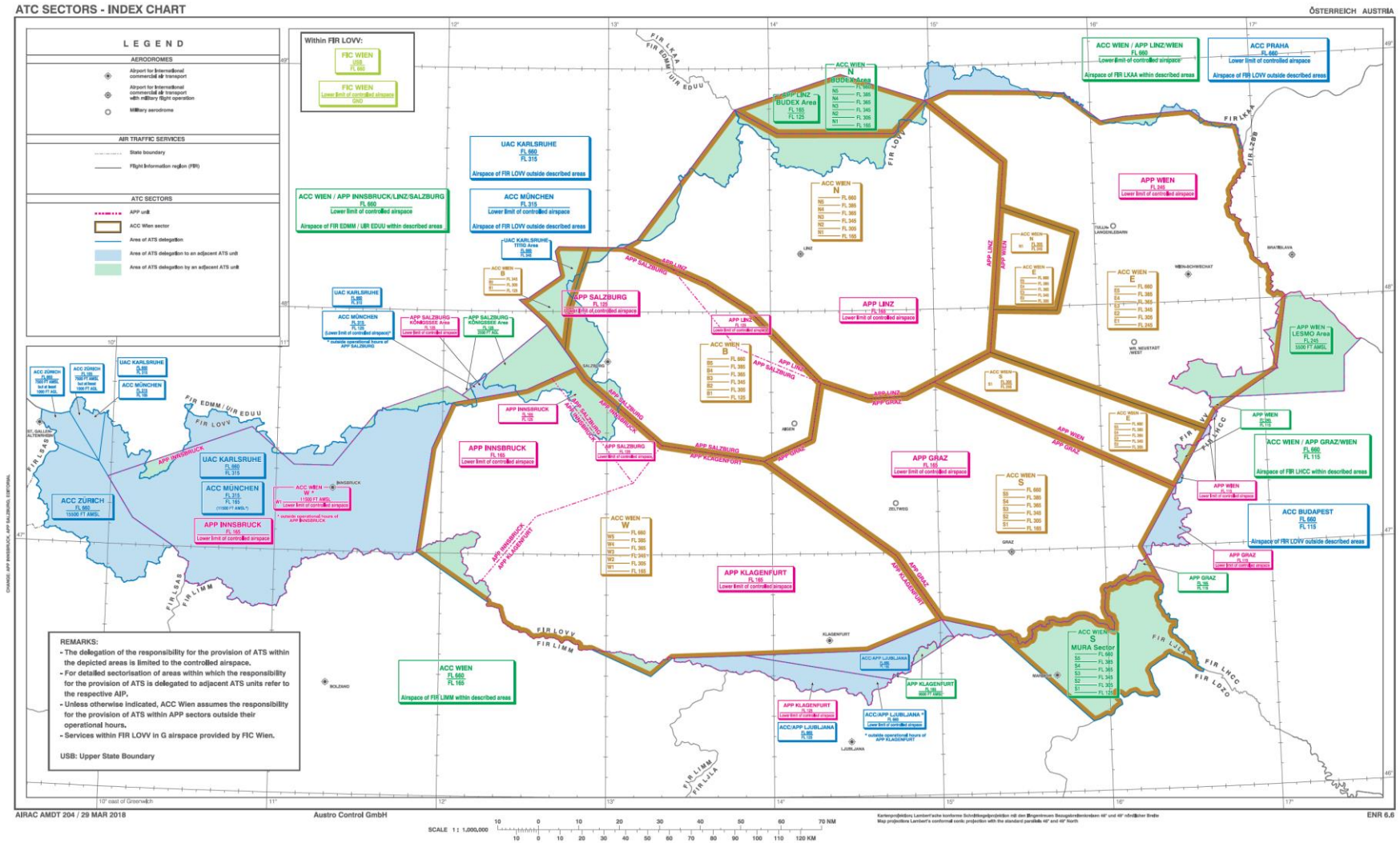

Figure 3: Geographical description of the Austrian airspace.

Another, more complicated, sector configuration is 10A1, whose ten sectors are the following:

- B15, formed by all the elementary volumes from ACC WIEN B.
- N12, formed by the elementary volumes from N1 and N2.
- N35, formed by the elementary volumes from N3, N4 and N5.
- E13, formed by the elementary volumes from E1, E2 and E3.
- E45, formed by the elementary volumes from E4 and E5.
- S12, formed by the elementary volumes from S1 and S2.
- S35, formed by the elementary volumes from S3, S4 and S5.
- W12, formed by the elementary volumes from W1 and W2.
- W3, formed by W3.
- W45, formed by W4 and W5.

The sector configurations considered in this application are the ones scheduled for the 12th of June 2018, between 12:00 and 20:00. These configurations and their activation and deactivation times are shown in

Table 1. The configurations of interest are highlighted in red; namely, configurations 10A1, 9A1, 8S, 7WB1, and 6WB1.

Active hours	Sector configuration
00:00 – 04:00	2A
04:00 – 04:30	5WB2
04:30 – 05:00	6WB1
05:00 – 08:00	7A
08:00 – 08:30	8S
08:30 – 09:00	9A1
09:00 – 10:00	10A1
10:00 – 11:00	11A1
11:00 – 14:30	10A1
14:30 – 17:00	9A1
17:00 – 18:00	8S
18:00 – 19:30	7WB1
19:30 – 20:00	6WB1
20:00 – 20:30	5WB2
20:30 – 21:30	4G
21:30 – 22:00	3F
22:00 – 23:59	2A

Table 1. Standard sector configuration schedule for 12th of June 2018.

4.1.2 Flights

The historical traffic data has been retrieved from Eurocontrol's R&D Data Archive[1]. To simplify the application, we consider the flight plan's data, not the actual data: the positions of airborne aircraft at 12:00, the nominal take-off times, and the nominal routes to be followed are the ones given in their flight plans.

The traffic considered in the application consists of aircraft airborne at 12:00 or expected to take-off in the next 8 hours (including the uncertainty in the take-off time) which plan to cross the Austrian airspace plus a surrounding area of 50 NM. In this way, it is contemplated the possibility that some aircraft, flying close to the airspace of interest may be deviated into it because of the convective weather.

A total number of 2542 flights are considered in this application: 393 flights are airborne at 12:00, and 2149 flights are expected to depart in the next 8 hours. Their planned routes are shown in Figure 4.

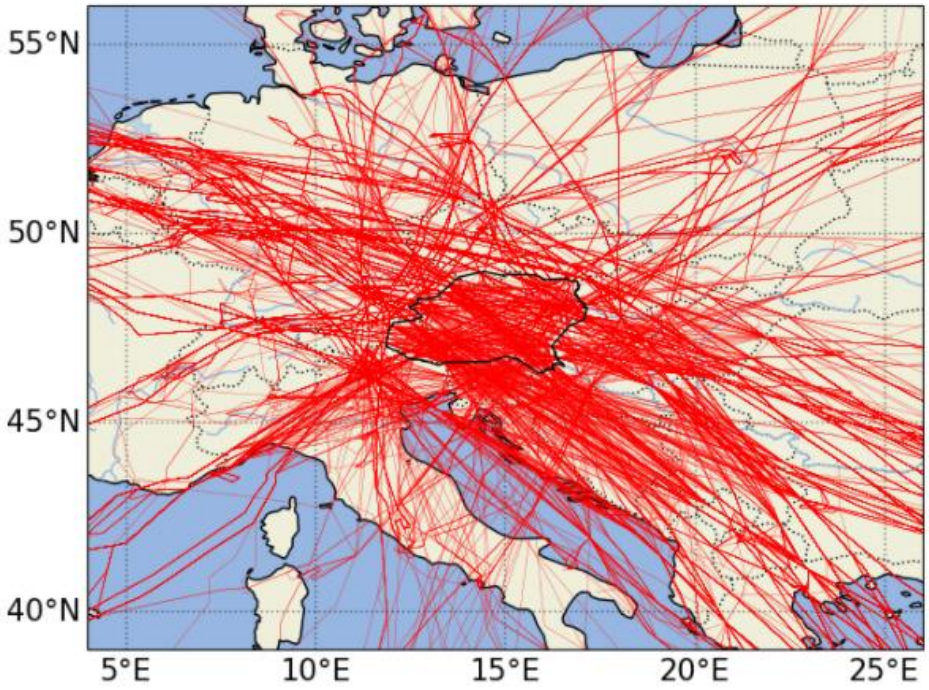

Figure 4. Planned routes of the flights considered in the application.

[1] https://www.eurocontrol.int/dashboard/rnd-data-archive

4.1.3 Weather

The three probabilistic weather forecasts considered in this application, one ensemble nowcast and two Ensemble Prediction Systems (EPS), are described next.

Ensemble Nowcast

Generated by AEMET, as described in Deliverable 3.1 [10]. We consider the last available nowcast at the moment of the prediction; in this application, the one generated at 11:45. It has been interpolated every 5 minutes and processed to identify the convective cells (at 38 dBz) and enlarged with a safety margin (13.5 NM). A common cloud top height for all the nowcast coverage area has been also provided: the flights can overfly them with a margin of 5000 ft. The number of members is 15, and they are statistically independent among them. An example, corresponding to a prediction for 12:30, generated at 11:45, is depicted in Figure 5. The storm cells, already enlarged with a safety margin of 13.5 NM, are represented in red. The transparency in a particular location represents the number of members that predict a storm cell to be in that very location (less transparent, more members).

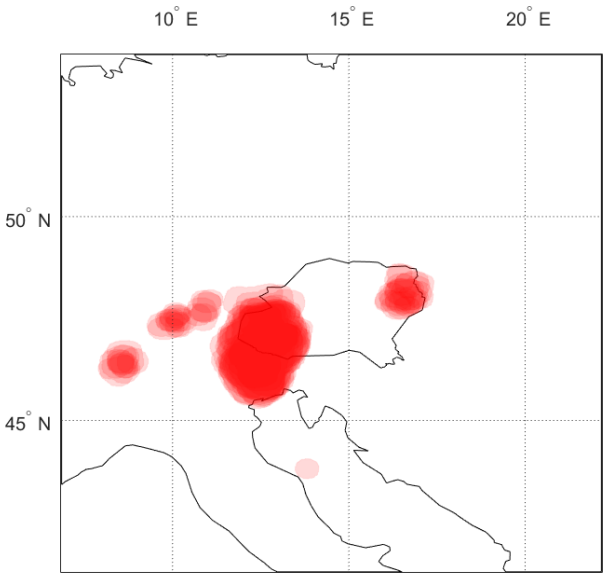

Figure 5. Nowcast generated at 11:45, prediction for 12:30.

COSMO-D2-EPS

Limited-area, high-resolution EPS. Purchased from the Fraunhofer Institute for Energy Economics and Energy System Technology (IEE). The number of members is 20, and they are statistically independent among them. The convection indicators identified in Deliverable 3.1 [10], Total Totals Index and Total Precipitation, could not been retrieved from the information stored by Frahunhofer IEE. Alternatively, two other indicators have been taken into consideration: Lifted Index and Precipitation Intensity.

Convective areas are identified when the Lifted Index is less than -4, and the Precipitation Intensity is above 5 mm/hour.

Also, a transition zone with unrealistic gradients has been identified in the contour of COSMO-D2-EPS coverage area, resulting from its boundary conditions during its generation. As a result, the outer 25 grid points on each side (about 50 km) have been discarded, being the coverage area of COSMO slightly downsized.

In this application, the last available COSMO-D2-EPS is the one generated at 09:00. It has been interpolated every 15 minutes and processed to identify the convective areas.

ECMWF-EPS

Global EPS from the European Centre for Medium-Range Weather Forecasts (ECMWF). Downloaded by AEMET. The number of members is 50, and they are statistically independent among them. Convective areas are identified when the Total Totals is above 44 K, and the Convective Precipitation is above 0.

In this application, the last available ECMWF-EPS is the one generated at 00:00. It has been interpolated every 15 minutes and processed to identify the convective areas.

4.2 Entry and occupancy counts

Next, the entry and occupancy counts, derived from the predicted trajectories, are presented. For the sake of brevity, only results for sector B15 are shown; to keep consistency, weather reduced capacities and congestion are also shown for this same sector. The values considered for the SKIP-IN and SKIP-OUT parameters are 1 and 30 minutes, respectively.

The graphical representation of the results has been chosen to facilitate their analysis, not for operational purposes. The most adequate graphical displays for proper output visualization for the FMP will be decided at the end of the project.

Entry count

Figure 6 shows the entry count $E_{sj}^{[k]}$ for time periods between 12:00 and 20:00 with $\delta t = \Delta t = 1$ hour. Just one weather-ensemble member is considered: $k = 2$ for the Nowcast (between 12:00 and 13:00) and $k = 1$ for COSMO-D2-EPS (between 13:00 and 20:00).

The entry count is represented as a heatmap, where the color for each count value represents the probability of obtaining that particular value; the darker the color, the higher the probability. The 5th and 95th percentiles are represented as small black squares, and the 50th percentile (i.e., the median) as a small black rhombus. The median represents the middle value, and the difference between the two percentiles is a measure of the dispersion.

Since only one weather-ensemble member is considered at each time period, the probabilistic distributions are the result of the other two uncertainty sources: the operational uncertainty linked to the storm avoidance strategy and the uncertainty in the initial conditions of the trajectories. The median takes values between 20 and 45 flights per hour, approximately, and the dispersion goes between 6 and 12.

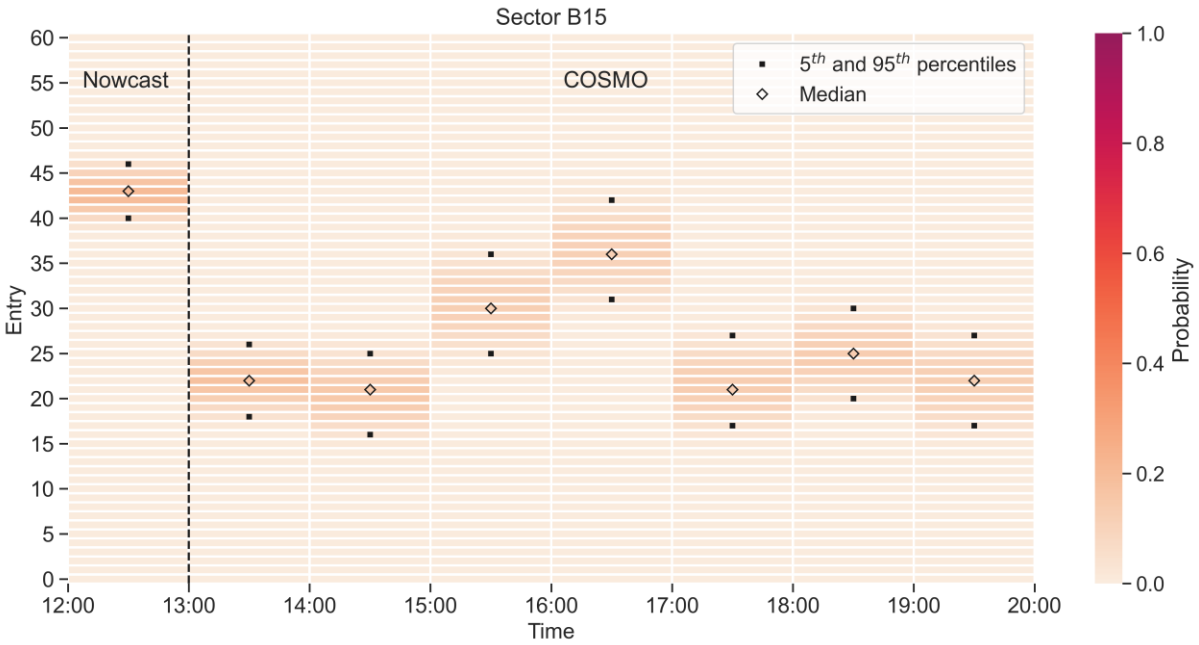

Figure 6. Entry count for member 2 of the Nowcast and member 1 of COSMO; $\delta t = \Delta t$ =1 hour.

The aggregated entry count, for all weather-ensemble members, E_{sj}, is shown in Figure 7. This is the probabilistic entry forecast that would be presented to the FMP. The time periods in this figure are defined with δt =20 minutes and Δt =1 hour, according to usual practice. The median takes values similar to those shown before, between 20 and 55; however, the dispersion now goes between 8 and 16, showing that considering the meteorological uncertainty increases the spread of the prediction.

Notice that, although the periods 12:20-13:20 and 12:40-13:40 have been computed with the modified procedure (because they include the transition time, T_T), their results are in line with the results from the other time periods, obtained with the general procedure. Therefore, this modified procedure seems to be appropriate.

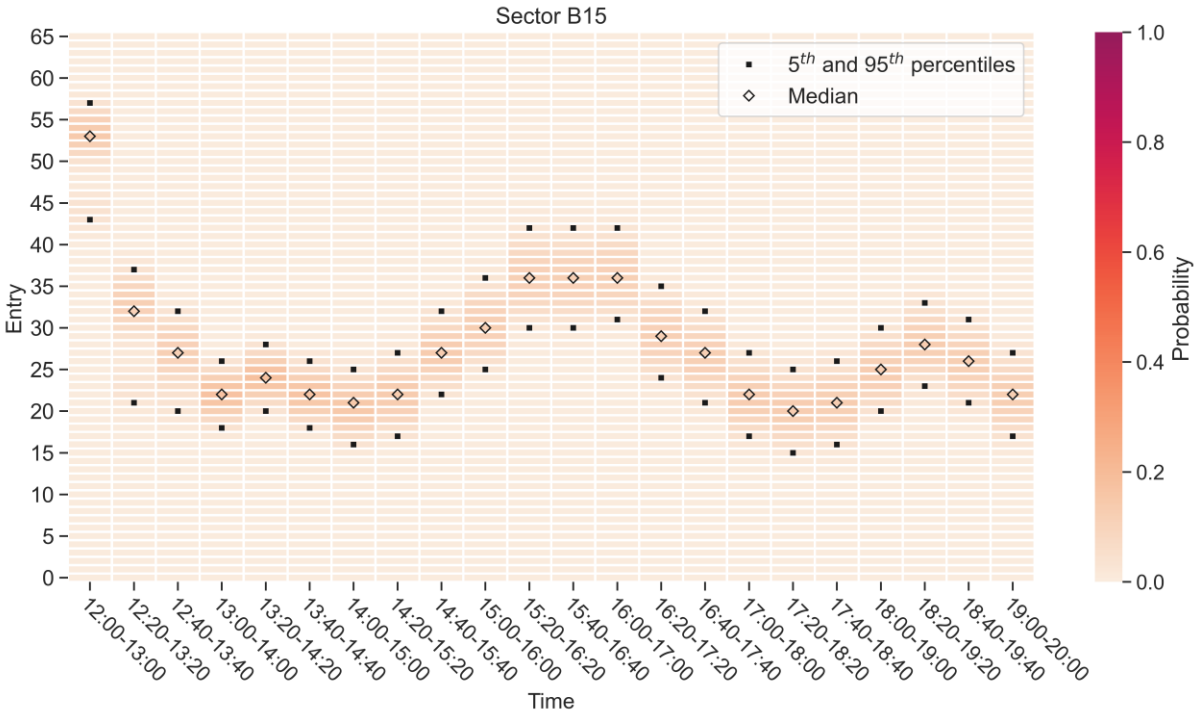

Figure 7. Aggregated entry count; δt =20 minutes, Δt =1 hour.

Occupancy count

Figure 8 shows the occupancy count $O_{sj}^{[k]}$ for time periods between 12:00 and 13:00 with $\delta t = \Delta t$ =1 minute, according to usual practice. Because the occupancy count is measured over such very short time periods, predictions with a lead time larger than one hour are not presented. The weather-ensemble member $k = 1$ of the Nowcast is considered. The median takes values between 4 and 15 flights, with a clear peak between 12:10 and 12:15. The dispersion goes between 0 and 5, clearly growing as the time horizon increases.

The aggregated occupancy count, for all weather-ensemble members, O_{sj}, is displayed in Figure 9. Again, this is the probabilistic occupancy forecast that would be presented to the FMP. The median is similar to the one presented in the previous figure. Once more, the dispersion is larger when the meteorological uncertainty is considered; now, it starts growing earlier and reaches larger values, up to 7 flights.

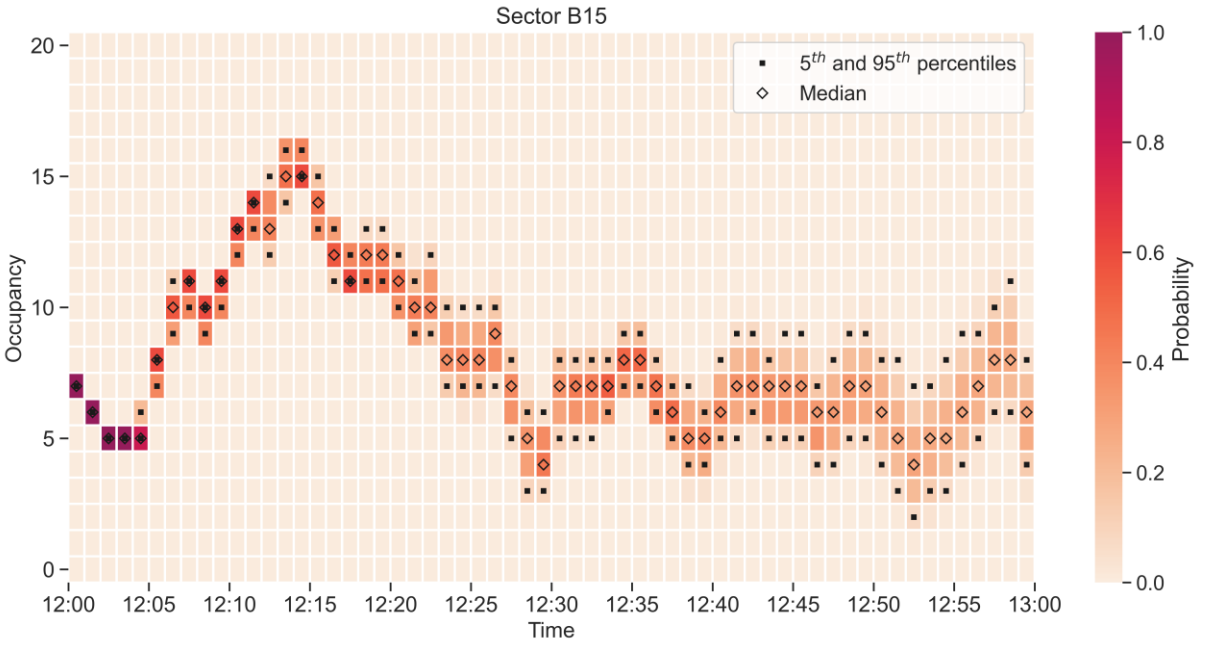

Figure 8. Occupancy count for member no. 1 of the Nowcast; $\delta t = \Delta t$ =1 minute.

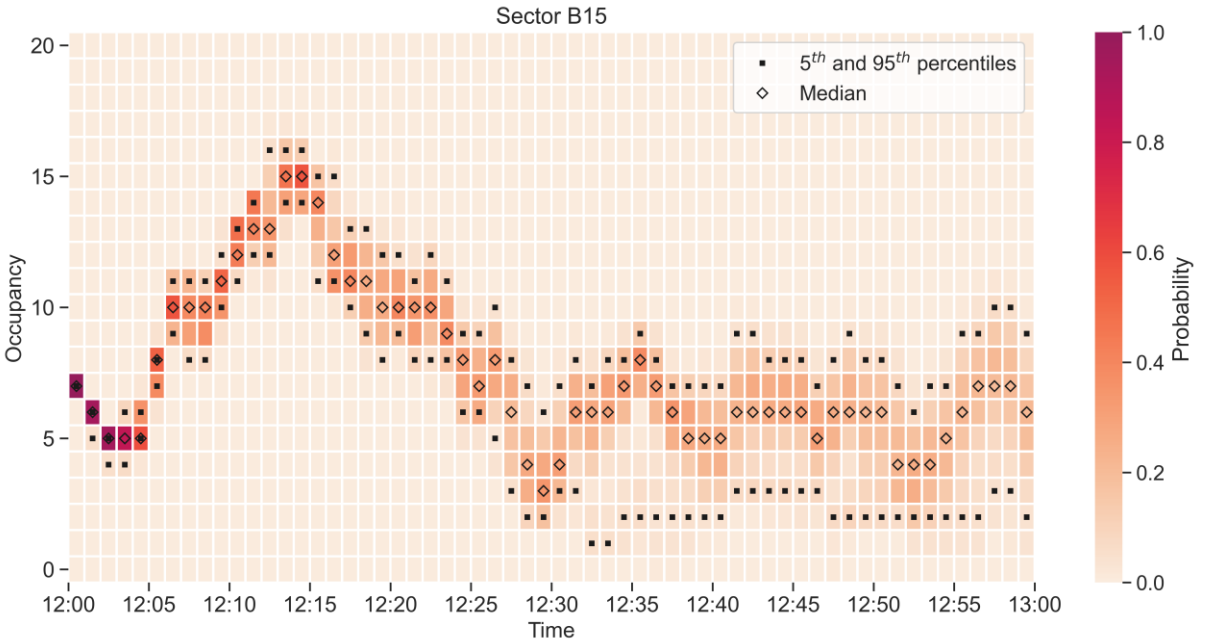

Figure 9. Aggregated occupancy count; $\delta t = \Delta t$ =1 minute.

4.3 Reduced weather capacities

The capacity reduction as a function of time, $ASCR_s^{[k]}(t)$, obtained between 12:00 and 13:00 for Nowcast member five, is presented in Figure 10. The ASCR significantly decreases as time progresses, going from approximately 0.8 to 0.3. The mean ASCR for the first hour (period $j = 1$), $\overline{ASCR}_{s1}^{[k]}$, which is derived from $ASCR_s^{[k]}(t)$, see Eq. (17), and represents the average state of the sector for this hour, is also shown in this figure.

The capacity reduction as a function of time, for all weather members, $ASCR_s(t)$, between 12:00 and 20:00, is presented in Figure 11. It has been obtained from Nowcast for the first hour and from COSMO-D2-EPS onwards. This figure is analogous to those presented in Deliverable 6.1 [11]. Regarding the median, it can be seen that the capacity starts with some reduction, it progressively further decreases during the first hour, remains at low values until 14:30, and then fully recovers, although for some weather members significant reductions may be present (as indicated by the heatmap and the 5th percentile).

The mean ASCR for time periods with δt =20 minutes and Δt =1 hour, is shown in Figure 12. This parameter can be seen as a low-pass frequency filter of $ASCR_s(t)$, which smooths its evolution. Now, it can be more clearly seen the capacity reduction, with a minimum at period 13:00-14:00, and its posterior recovery.

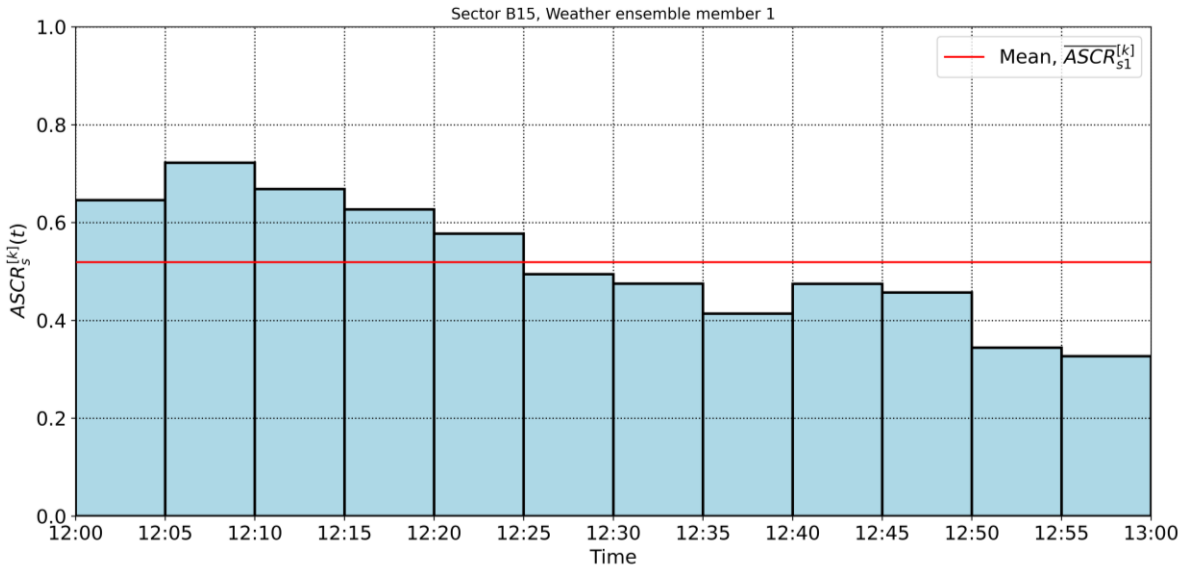

Figure 10. ASCR for the first hour and for Nowcast-member number five.

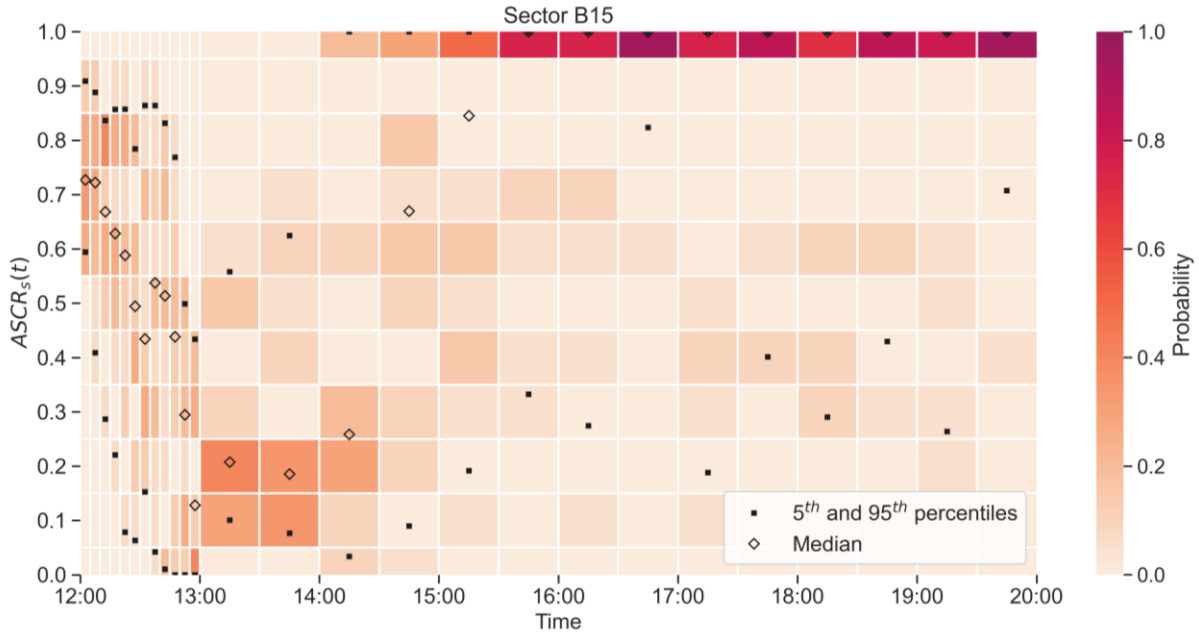

Figure 11. ASCR for all weather members.

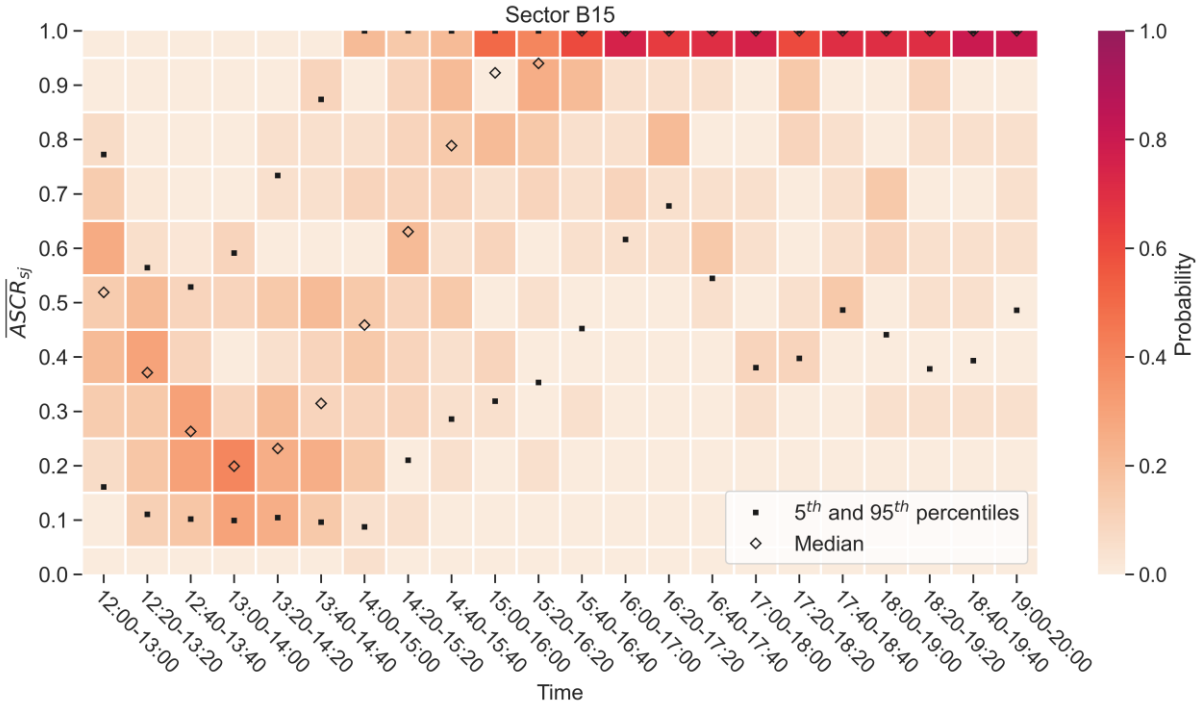

Figure 12. Mean ASCR; δt =20 minutes, Δt =1 hour.

The weather-dependent MV, Wx_MV_{sj}, is shown in Figure 13 for time periods between 12:00 and 20:00 and with δt =20 minutes and Δt =1 hour. Figures Figure 12 and Figure 13 are very much alike, since Wx_MV_{sj} is just the product of the mean ASCRs and the nominal MV, see Eq. (20). The nominal MV is also represented in this figure as a blue line.

Figure 14 represents the weather-dependent OTMV, Wx_OTMV_{sj}, for the first hour and with $\delta t = \Delta t$ =1 minute. It has been obtained by multiplying the ASCRs and the nominal sustained OTMV, see Eq. (21). Since the ASCRs are provided every 5 minutes during the first hour, then Wx_OTMV_{sj} remains constant during these 5-minute intervals. It can be observed that it is progressively reduced during this first hour. Notice also that, between 12:35 and 13:00, the 5th percentile is zero, meaning that for some weather-ensemble members this sector is completely blocked.

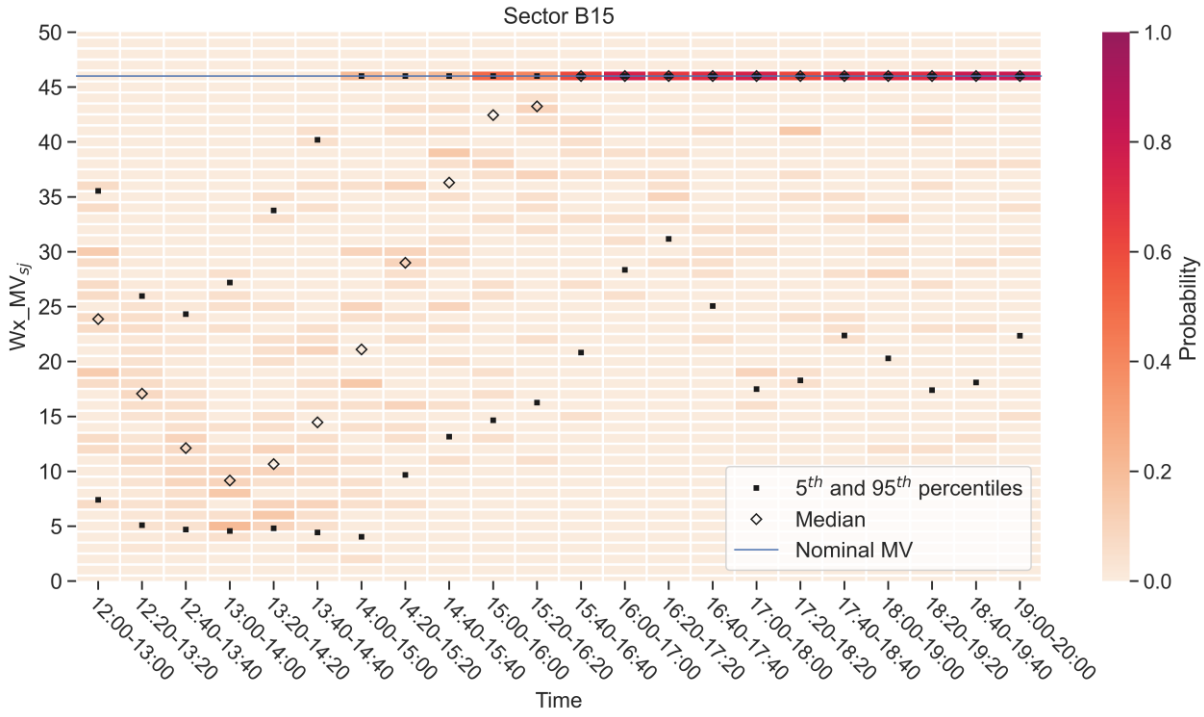

Figure 13. Weather-dependent MV; δt =20 minutes, Δt =1 hour.

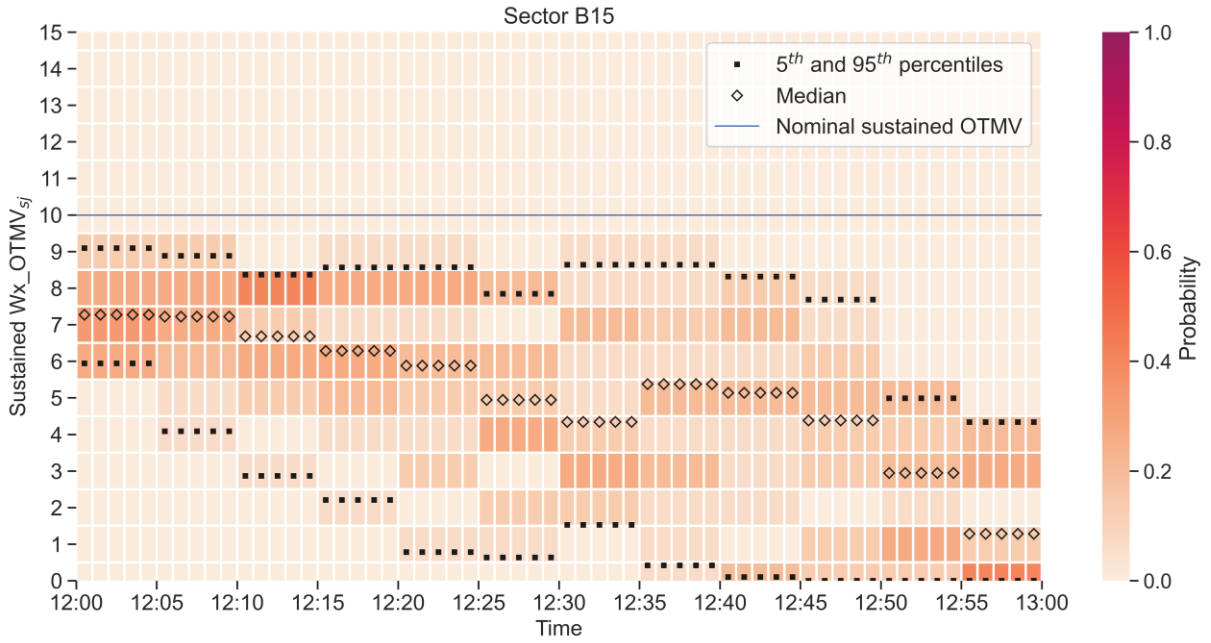

Figure 14. Weather-dependent sustained OTMV; $\delta t = \Delta t$ =1 minute.

4.4 Congestion

Entry overload

The absolute overload of the entry count is represented in Figure 15 for time periods between 12:00 and 20:00, with δt =20 minutes and Δt =1 hour. The overload is certainly positive for the earliest periods, which is a consequence of high counts and reduced capacities, as shown in Figures Figure 7 and Figure 13. Afterwards, the overload is reduced. For the latter periods, the median is distinctly negative but an overload is still possible since the 95th percentile is above zero. Notice that the dispersion is quite large, and the median is much closer to the 5th percentile than to the 95th one.

The relative overload is displayed in Figure 16. Again, it is quite large for the first periods and smaller for the last ones. Notice that the vertical axis has been capped at 3.0 and that the 95th percentile is beyond that number for periods between 12:00 and 15:00. It is peculiar and worth mentioning that the dispersion of the relative overload is smaller for latter periods.

Relative overloads of 0.9, 1.0, and 1.1 are highlighted in the figure, as they will be later used when determining the congestion status of the sector. It is remarkable that these three lines are quite close among them, in comparison with the dispersion and variability of the relative overload.

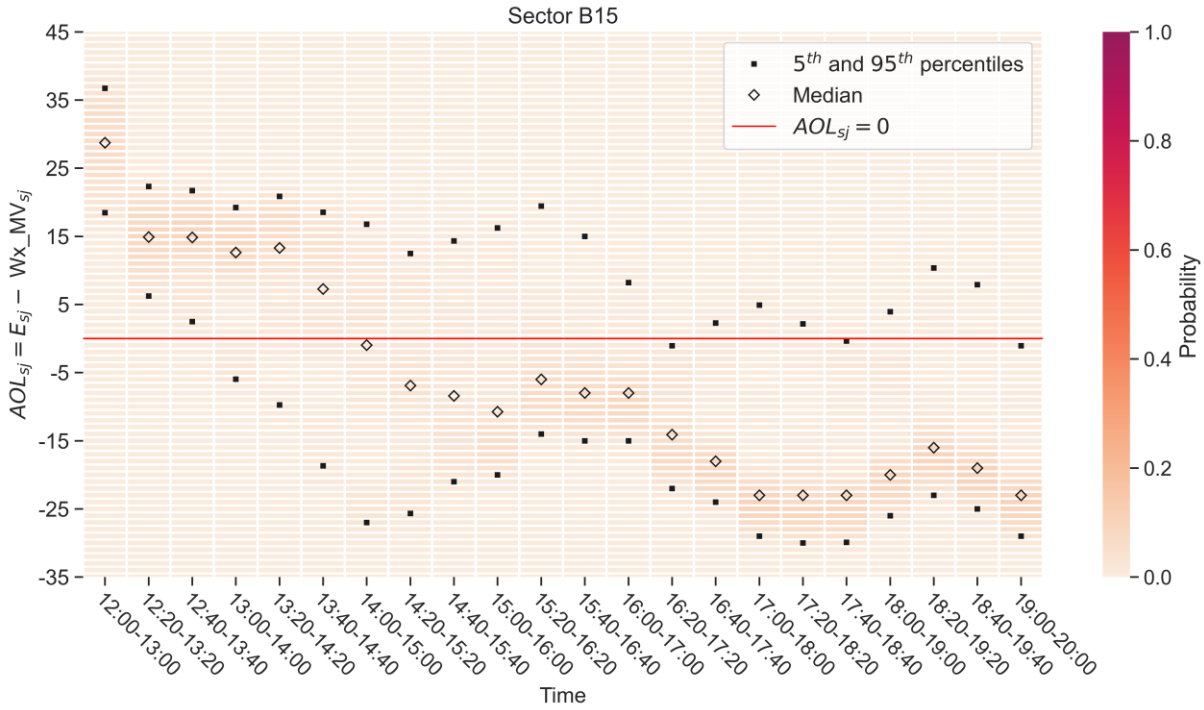

Figure 15. Entry absolute overload; δt =20 minutes, Δt =1 hour.

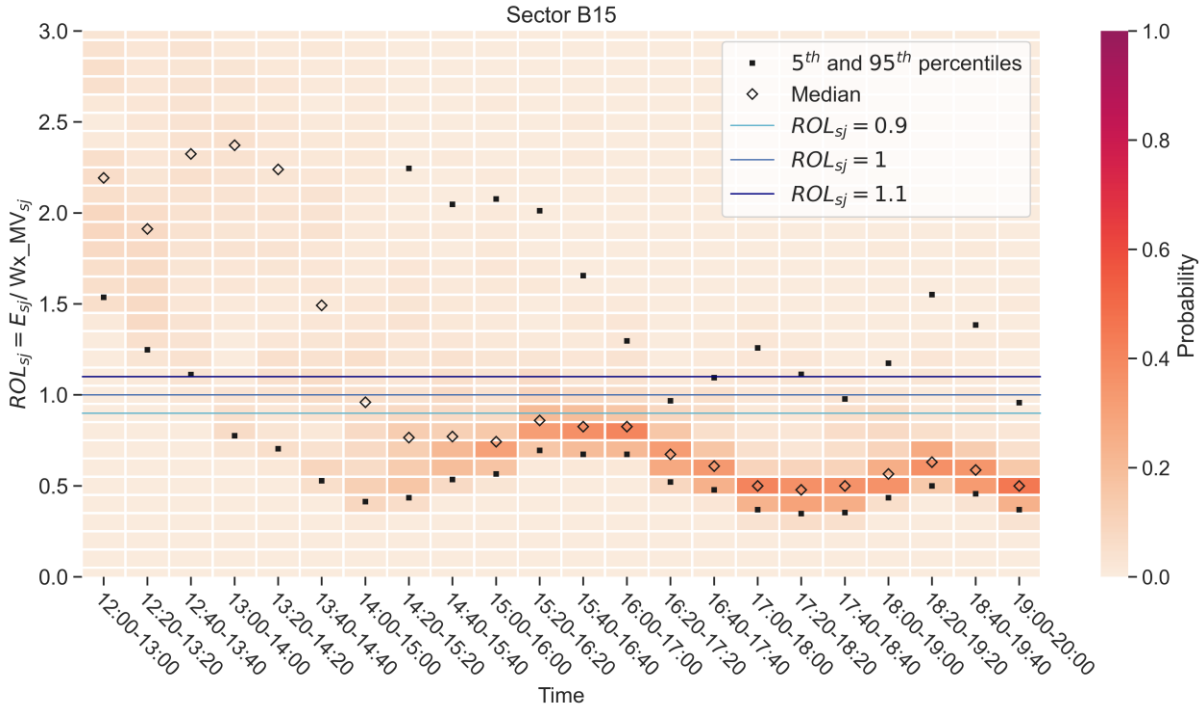

Figure 16. Entry relative overload; δt =20 minutes, Δt =1 hour.

Occupancy overload

The absolute overload of the occupancy count is represented in Figure 17 for the first hour, with $\delta t = \Delta t = 1$ minute. The overload is positive for almost all periods. The peak between 12:10 and 12:15 corresponds to the peak in the occupancy count, see Figure 9, although here it is less noticeable because the capacity decreases along time, see Figure 14. The dispersion grows as time progresses.

The relative overload is shown in Figure 18. Notice that again the vertical axis has been capped and that the 95th percentile is beyond the limit for several periods. The dispersion is quite large, especially when the capacity is very small, see Figure 14. When the sector is blocked and the capacity is zero for some weather-ensemble members, then Eq. (28) does not longer hold. In that particular case, it is considered that the relative overload is infinite.

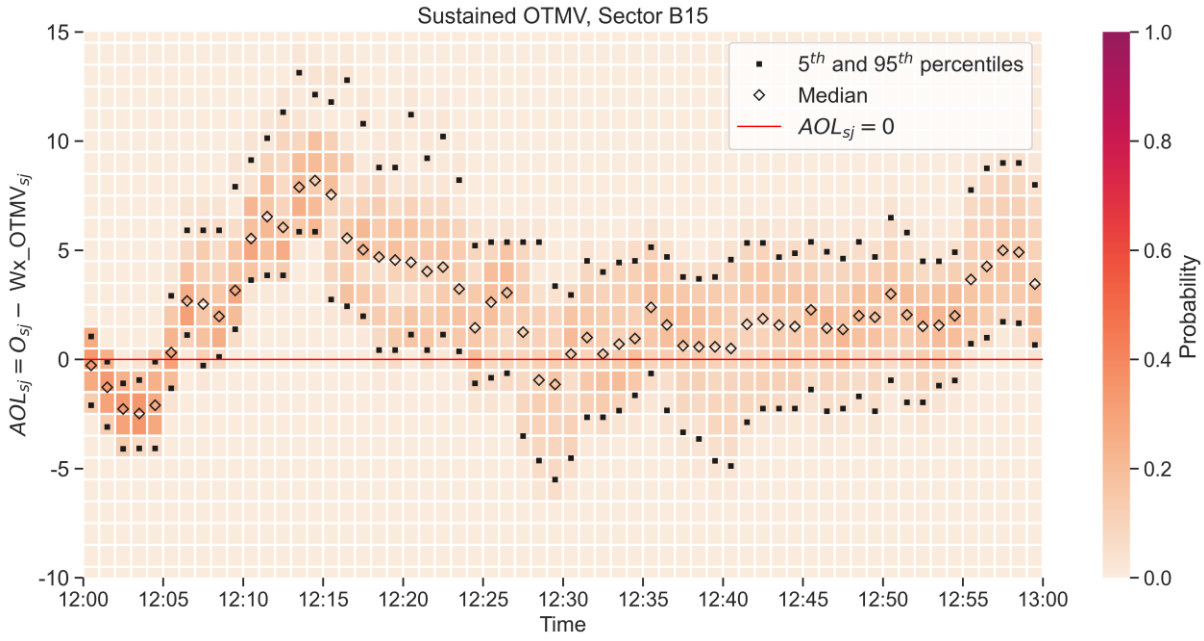

Figure 17. Occupancy absolute overload; $\delta t = \Delta t = 1$ minute.

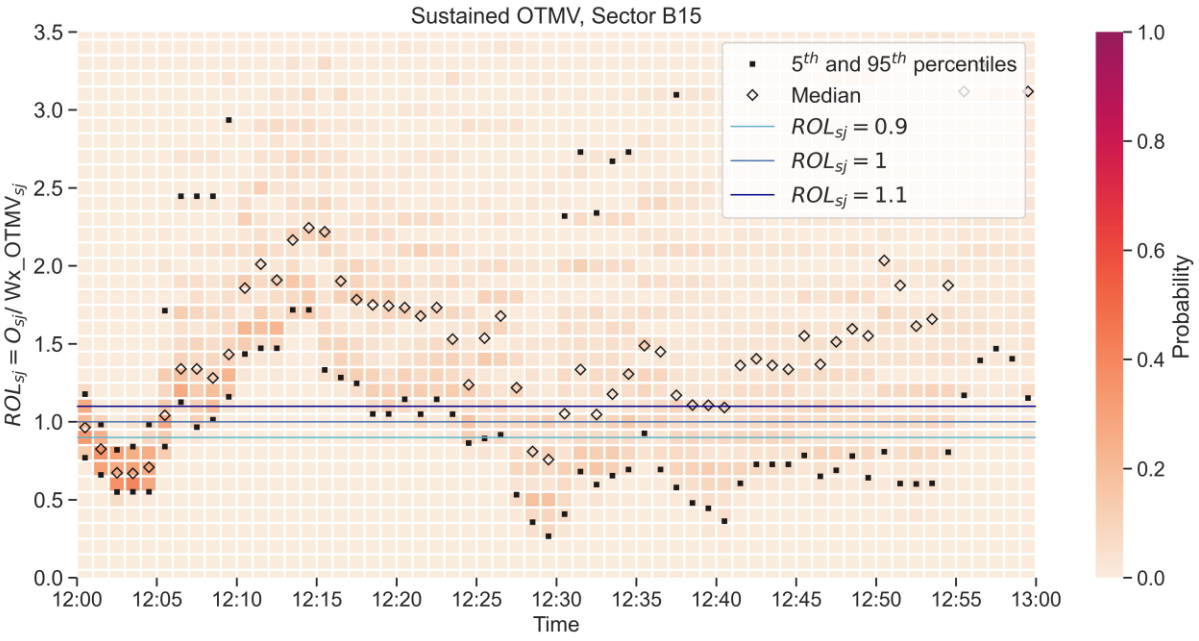

Figure 18. Occupancy relative overload; $\delta t = \Delta t$ =1 minute.

Output visualization example

One of the specific objectives of the FMP-Met project is to define the proper output visualization of the probabilistic traffic information previously analyzed. In WP2 various tools and different color schemes were proposed (Deliverable 2.1 [1]).

Although this task is to be done in WP7, next, to conclude this deliverable, an example is included to show how the data presented to the FMP may look like. The tool considered is the *Traffic Volume Monitor* and the color scheme is the following:

- Green: if $P[TF_{sj} \leq 0.9Wx\_Cap_{sj}] \geq 95\%$
- Yellow: if $P[TF_{sj} \leq Wx\_Cap_{sj}] \geq 95\%$ AND $P[TF_{sj} > 0.9Wx\_Cap_{sj}] \geq 5\%$
- Orange: if $P[TF_{sj} \leq 1.1Wx\_Cap_{sj}] \geq 95\%$ AND $P[TF_{sj} > Wx\_Cap_{sj}] \geq 5\%$
- Red: if $P[TF_{sj} > 1.1Wx\_Cap_{sj}] \geq 5\%$

This scheme, based on the probability that the traffic flow exceeds a multiple of the weather-dependent capacity, can be expressed as follows in terms of the relative overload:

- Green: if $P[ROL_{sj} \leq 0.9] \geq 95\%$ (i.e., if 95th percentile is at or below 0.9)
- Yellow: if $P[ROL_{sj} \leq 1] \geq 95\%$ AND $P[ROL_{sj} > 0.9] \geq 5\%$ (i.e., if 95th percentile is above 0.9 and at or below 1)
- Orange: if $P[ROL_{sj} \leq 1.1] \geq 95\%$ AND $P[ROL_{sj} > 1] \geq 5\%$ (i.e., if 95th percentile is above 1 and at or below 1.1)
- Red: if $P[ROL_{sj} > 1.1] \geq 5\%$ (i.e., if 95th percentile is above 1.1)

This color scheme is applied to the entry relative overload.

The status of all the sectors that make up sector configuration 10A1 is shown in Figure 19, for time periods between 12:00 and 20:00, with δt =20 minutes and Δt =1 hour. All sectors present unacceptable traffic loads for some periods. Some sectors are overloaded at the beginning and then they recover (e.g., W45, W3, and W12), and other sectors are overloaded between 13:00 and 17:00, approximately. The status of sector B15 can be easily deduced from Figure 16, just by checking the position of the 95th percentile and the reference lines 0.9, 1.0 and 1.1.

The status of the sector configuration is determined from the color state of its constituent sectors: green if the traffic load is acceptable for all sectors, yellow if it is high for at least one sector, orange if it is very high for at least one sector, and red if it is unacceptable for at least one sector. In this application, the sector configuration 10A1 is unacceptable for all time periods.

According to Figures Figure 15 and Figure 16, the probability distributions of the overload can be asymmetrical and heavy-tailed. Therefore, using the 95th percentile as the only parameter in the criteria to determine the overload status of the sector may be insufficient. An impact matrix approach, as the one proposed in Deliverable 2.1 [1], may be a better approach. As already mentioned, an evaluation of different criteria will be performed at the end of the project.

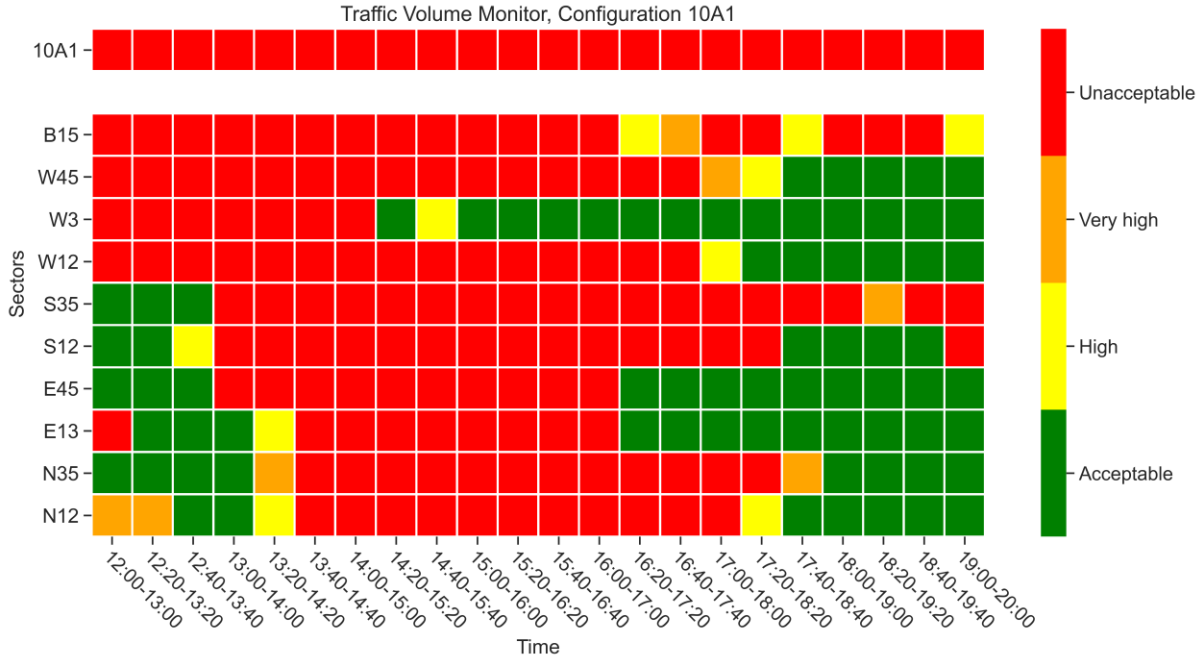

Figure 19. Traffic Volume Monitor for sector configuration 10A1; δt =20 minutes, Δt =1 hour.

5 Conclusions

This document has presented methodologies to obtain the stochastic distributions of the traffic counts and their differences with weather-dependent capacities when convective weather is forecasted. These methodologies rely on the probabilistic aircraft trajectories returned by the trajectory predictors developed in WP 4 and the weather-dependent capacities derived from the capacity reductions determined by WP 6. These methodologies consider the usage of different weather products, the presence of multiple uncertainty sources and their statistical correlations.

The developed methodologies are based on the determination of probability mass functions, from the trajectories and reduced capacities, and their posterior processing. This approach produces exact probability distributions from the inputs (i.e., they are as exact as the inputs are). Alternative methodologies, based on a sampling of the inputs, could have been developed, but they have been discarded because they introduce simplifications and degrade the output probability distributions.

The developed methodologies have been applied to a scenario based on a historical situation over the Austrian airspace on a day with significant convection. Probability distributions, and their evolution along time, of entry and occupancy counts, weather-dependent capacities, and entry and occupancy overloads have been obtained.

Different statistics can be determined from the probability distributions as, for example, the median and percentiles. These distributions and their statistics allow to observe the expected evolution of the different traffic parameters and their stochastic nature. For example, the dispersion of the occupancy count clearly grows during the first hour, increasing its uncertainty as time progresses.

Storms can evolve very fast and, consequently, also the sector capacity ratios provided by the methodologies from WP 6. Since the occupancy count and the weather-dependent occupancy traffic monitoring value are determined over short time periods, they can capture this dynamicity. However, the entry count and the weather-dependent monitoring value are usually determined for time periods with a duration of one hour, and they may miss these quick changes. One possible solution to overcome this is to determine the entry count and the monitoring values for shorter time periods. The developed methodologies do not require any alteration if the durations are modified, but the air navigations services providers should define nominal monitoring values for shorter time periods as they cannot be simply scaled to the period's duration.

Results have shown that the probability distributions of the overload can be asymmetrical and heavy-tailed. Therefore, it seems convenient the overload status to be defined not only by one parameter, but by several parameters that better reflect the shape of the distributions. This is to be addressed in WP 7, where different overload criteria will be evaluated, and the most useful graphical displays for the FMP will be identified.

6 References

[1] "FMP-Met Deliverable 2.1, Concept of Operations for Weather-Dependent Probabilistic Flow Management," Edition 00.02.00, December 2020.

[2] “TBO-Met Deliverable 5.1, Methodology to assess the uncertainty of sector demand,” Edition 01.01.00, March 2017.

[3] "FMP-Met Deliverable 4.1, Trajectory prediction under adverse weather scenarios," Edition 00.01.00, May 2021.

[4] A. M. Mood, F. A. Graybill and D. C. Boes, Introduction to the theory of statistics, 3rd ed., McGraw-Hill Inc., 1974.

[5] C. M. Grinstead and J. L. Snead, Introduction to probability, 2nd revised ed., American Mathematical Society, 1997.

[6] M. D. Springer, The Algebra of Random Variables, John Wiley & Sons Inc., 1979.

[7] S. Gillies, "The Shapely User Manual," 27 September 2020. [Online]. Available: https://shapely.readthedocs.io/en/stable/manual.html#id25. [Accessed 19 July 2021].

[8] Wiki, "GEOS," 16 June 2021. [Online]. Available: https://trac.osgeo.org/geos. [Accessed 19 September 2021].

[9] M. Davis, "JTS Technical Specifications," March 2003. [Online]. Available: https://github.com/locationtech/jts/raw/master/doc/JTS%20Technical%20Specs.pdf. [Accessed 19 September 2021].

[10] "FMP-Met Deliverable 3.1, Nowcast and EPS Forecast Products," Edition 00.02.00, December 2020.

[11] "FMP-Met Deliverable 6.1, Forecast of sector complexity and airspace capacity reduction in multi-sector scenarios," Edition 00.01.00, October 2021.

[12] P. S. Bradley, K. P. Bennett and A. Demiriz, "Constrained K-Means Clustering," MSR-TR-2000-65, Microsoft Research, 2000.

[13] "AIP Austria," [Online]. Available: https://eaip.austrocontrol.at/lo/210618/Charts/ENR/LO_ENR_6_6_en.pdf. [Accessed 30 June 2021].


UNIVERSIDAD DE SEVILLA
AEMet
Agencia Estatal de Meteorología
austro
CONTROL
CROATIA
CONTROL
LINKÖPING
UNIVERSITY
METEOSOLUTIONS
UNIVERSITÄT
SALZBURG
Universidad
Carlos III de Madrid